Analysis of sub-visible particles in complex injectable formulations

Sediq, A.S.

Chapter 6

A label-free method for cell counting and viability determination using flow imaging microscopy

A.S. Sediq[1], R. Klem[1], M.R. Nejadnik[1], P. Meij[2], W. Jiskoot[1,*]

[1] Division of Drug Delivery Technology, Cluster BioTherapeutics, Leiden Academic Centre for Drug Research (LACDR), Leiden University, Leiden, The Netherlands

[2] Department of Clinical Pharmacy and Toxicology, Leiden University Medical Center, Leiden, The Netherlands

Manuscript in preparation

Abstract

Two quality attributes of cell therapy products are cell concentration and percentage of viable cells. Despite the availability of techniques to determine cell concentration and viability, there is a need for label-free, robust and user-friendly techniques. In this study we have investigated the potential of two flow imaging microscopy (FIM) techniques (Micro-Flow Imaging (MFI) and FlowCAM) to determine cell concentration and viability. For this goal we have exposed B-lineage acute lymphoblastic leukemia (B-ALL) cells of 2 different donors to ambient conditions, in order to induce cell death. Samples were taken at different days and measured with MFI, FlowCAM, hemocytometry and automated cell counting. Dead and live cells from fresh B-ALL cell suspension were fractionated by flow cytometry in order to derive filters based on morphological parameters of separate cell populations with MFI and FlowCAM. The filter sets were used to assess the concentration of viable cells in the measured samples. All techniques gave fairly similar cell concentration values over the whole incubation period. However, MFI showed to be superior with respect to precision. Both FIM methods were able to provide similar results for viability as the conventional methods (hemocytometry and automated cell counting). Altogether, our investigation shows that FIM-based methods may be advantageous over conventional methods, as FIM measures much larger sample volumes, does not require labeling, is less laborious and provides images of individual cells. The latter asset we have successfully used to determine viability, but can potentially be employed to distinguish early stages of cell death and different cell types in a heterogeneous cell sample.

Introduction

Cell therapy products (CTPs) are receiving increasing attention by the pharmaceutical industry because of their demonstrated potential for use in treatment of a variety of diseases, such as cancers, viral infections, and autoimmune disorders[1,2]. The quality of CTPs relies, among others, on the viability of the cells. During production, cells used for cell therapy may undergo different process steps, such as harvesting, purification, genetic manipulation, expansion, freezing and thawing[3]. These procedures, as well as other treatments, such as transport[4] and storage in infusion medium/solution[5], and even the administration to the patient [6], can induce different types of stresses to the cells and potentially affect cell viability. While there are some regulations on what properties of CTPs should be tested[7], quick testing of viability prior to administration to the patient is often neglected. As a result, changes in product quality that might occur between production and administration could remain undetected.

Two main techniques that are frequently applied to assess cell viability are hemocytometry[8] and flow cytometry[9]. The determination of cell viability with a hemocytometer is based on staining of the dead cells using dyes like eosin and trypan blue[8]. In a flow cytometer a laser beam is focused on a flowing liquid. Individual cells in the flow scatter the laser light and are detected by the system. The type, size and other characteristics of the cells determines the degree of the scattering. The forward scatter (FSC) and side scatter (SSC) provide information about cell size and granularity, respectively. Granularity level has been shown to be inversely related with cell viability[10]. Intrinsic fluorescence of the cells and/or fluorescence from a fluorescent label can also be detected[11]. Moreover, the use of fluorescently labeled antibodies directed against cell surface markers can aid in the evaluation of cell type and viability. Flow cytometry is known to be a very accurate and reproducible technique for cell viability tests. However, absolute cell concentrations are usually not easily obtained. In addition, the preparation and labeling of the cells can be time-consuming and expensive.

Hemocytometry is the currently the gold standard in the clinical practice for cell counting and viability determination. Whilst being a fast method, the method can be laborious and has certain weak points that could potentially harm the accuracy of the method. For example, the pipetting of the cell suspension and fitting the cover glass may disrupt the sample homogeneity at the cytometer surface. In addition, the method uses only a few microliters of the suspension for the actual counting of the (viable and non-viable) cells and extrapolates this number to a concentration unit of cells per milliliter. With respect to the quantity of cell suspension measured and the laborious nature of the method, automated cell counters provide improvement, especially for routine measurements, as they measure about 4x as much volume as a hemocytometer (0.4 vs. 0.1 µL). However, one should be

aware that non-cellular particles in the sample could be counted as a cell as well.
In this regard, less laborious, inexpensive techniques that allow for rapid and reliable counting of CTPs would be extremely beneficial for improving the success of CTPs in clinical practice. Emerging flow imaging microscopy (FIM) techniques may fulfill these needs. In these systems the sample flows through a flow cell where images are taken with a high-magnification digital camera. With the help of the dedicated instrument software, the quantity and several morphological parameters of the particles can be extracted from the images[12]. FIM can give valuable information about cells, without the need for labeling, and detect small changes in cell size and morphology which have been shown to be related to cell viability[13,14]. In addition, FIM techniques are generally easy and fast to perform.
One of these FIM techniques is Micro-Flow Imaging, which owes it popularity in this field mainly to its user-friendliness and robust operation. The application of MFI for cells is limited but not unexplored. For instance, Martin et al. have used MFI to study aggregation tendency of thawed hematopoietic stem cells[15]. A recent study of Farrell and coworkers used MFI to determine cell coverage and confluency on microcarriers used in culture-derived bioreactors[16]. Besides MFI, FlowCAM has been explored for its potential in biologic drug product development[17-19] and drug delivery systems (*Chapter 4*).
The aim of this study was to evaluate the performance of two FIM techniques, *i.e.*, Micro-Flow Imaging (MFI) and FlowCAM, in their ability to determine cell viability. Even though the devices are based on the same measurement principle, they differ in several aspects. The FlowCAM has a higher resolution and provides more particle parameters, whereas the MFI tends to provide a more accurate determination of particle concentration[19,20]. In the presented study, the two systems are used for the characterization of two cell lines and compared with hemocytometry and automated cell counting as well as with each other.

Materials and methods

Cell materials

B-lineage acute lymphoblastic leukemia (B-ALL) cells were used as model cells in this study. The cells were cultured from two different donors (ALL-CR and ALL-CM[21]; further referred to as cell line 1 and cell line 2) and provided by the Department of Hematology, Leiden University (LUMC, Leiden, the Netherlands). Cells were frozen in 60% v/v wash medium (BioWhittaker® Iscove's Modified Dulbecco's Medium (IMDM) 98.5% v/v, penicillin/streptomycin (Lonza) 1% v/v, HSA-20% 0.5% v/v) and a final concentration of 10% v/v HSA-20%, 10% v/v DMSO (LUMC, Leiden, the Netherlands) at a concentration of about $1 \cdot 10^7$ cells/mL and stored at -80˚C until the start of incubation experiments. After controlled thawing, washing and counting, cells were suspended in NaCl 0.9% m/v + HSA-20% 2% v/v at a concentration of 10^6 cells/mL and were exposed to the stress condition described

below.

Stress condition

The chosen stress condition in which the cells showed a clear decrease in, but not a total loss of viability, was incubation at ambient temperature for up to 8 days. The cell concentration and morphological parameters of each sample were analyzed at different days by using MFI and FlowCAM. For cell line 1 the measurements were performed at day 0, 1, 2, 4, 6 and 8. The study performed with the 2nd cell line served as a confirmative study and therefore the measurements at day 4 and 6 were not performed. In parallel, the cell concentration and number of viable cells in the same samples were determined with a hemocytometer and an automated cell counter. For the data analysis of both flow imaging microscopy techniques we only included particles detectable with the hemocytometer and the automated cell counter, *i.e.*, particles ≥4 µm.

Hemocytometry

Cell suspensions were diluted twofold with a trypan blue solution (0.4% (w/v) in 0.81% NaCl and 0.06% K_2HPO_4 (Bio-Rad, Hercules, California, USA)). Ten µL of the mixture was placed on a Bright-Line hemocytometer glass (Sigma-Aldrich, Steinheim, Germany), and analyzed by using a light microscope (Zeiss Axiostar Plus, Carl Zeiss Light Microscopy, Göttingen, Germany). Both viable (not stained) and non-viable (stained) cells were counted in 25 frames of the hemocytometer according to the manufacturer's recommendations and the percentage of viable cells to the total was calculated[22]. For each sample triplicate measurements were conducted.

Automated cell counting

Ten µL of the mixture prepared for the hemocytometry was introduced into the counting slide. Subsequently, the cell concentration and percentage of viable cells were measured by using a Bio-Rad TC20 Automated Cell Counter (Bio Rad, Hercules, California, USA). This procedure was repeated three times for each sample.

Micro-Flow Imaging (MFI)

In order to decrease the concentration of the cells and reduce the chance of detection of overlapping particles, samples were first diluted 4-fold with the particle free NaCl 0.9% m/v + HSA-20% 2% v/v . The diluted samples were analyzed by using a Micro Flow Imaging 5200 (Protein Simple, Santa Clara, CA, USA), with MFI View System Software (MVSS) Version 2. No filters were applied during the runs. The 100 µm silane coated flow cell was rinsed with flow of ultrapure water (18.2 MΩ.cm; dispensed by using a Purelab Ultra

water purification system (ELGA LabWater, Marlow, UK) and thereafter a background measurement was taken with particle free NaCl 0.9% m/v + HSA-20% 2% v/v. For the analysis, 0.50 ml of each sample was run at a flow rate of 0.17 mL/min. The data analysis was performed with MFI View Analysis.

Table 1: Morphological parameters used in this study and their descriptions asprovided by MVAS (MFI) and Visual SpreadSheet (FlowCAM).

Parameter	Unit	Description
Micro-Flow Imaging		
Equivalent circular diameter (ECD)	Microns	The diameter of a circle occupying the same area as the particle
Intensity mean	Intensity (0 – 1023)	The average intensity of all image pixels representing the particle
Intensity standard Deviation	Intensity (0 – 1023)	The standard deviation of the intensity of all pixels representing the particle
Circularity	No units (0 – 1)	The circumference of a circle with an equivalent area divided by the actual perimeter of the particle
Aspect ratio	No units (0 – 1)	The ratio of the minor axis length over the major axis length of an ellipse that has the same second-moment-area as the particle
FlowCAM		
Area based diameter (ABD)	Microns	The diameter based on a circle with an area that is equal to that of the particle
Symmetry	No units (0 – 1)	A measure of the symmetry of the particle around its center. If a particle is symmetric then the value is one.
Aspect ratio	No units (0 – 1)	The ratio of the width (the shortest axis of the particle) and length (the longest axis of the particle)
Circle fit	No units (0 – 1)	Deviation of the particle edge from a best-fit circle, normalized to the zero to one range where a perfect fit has a value of one.
Circularity	No units (0 – 1)	A shape parameter computed from the perimeter and the area. A circle has a value of one. Formula: $(4 \times \pi \times \text{Area}) / \text{Perimeter}^2$.

Suite (MVAS) Version 1.2. Table 1 summarizes the main morphological parameters provided by the MVAS and their descriptions. The size distribution of each sample was presented in equivalent circular diameter (ECD). Each sample was measured three times with MFI.

FlowCAM

The second flow imaging technique used in this study was a FlowCAM VS1 (Fluid Imaging Technologies, Yarmouth, ME, USA). After rinsing the FC50 flow cell with ultrapure water, 100 µL of each 4-fold diluted sample was run at a flow rate of 0.030 ml/min controlled by a C70 syringe pump. Images were taken with a Sony XCD-SX90 camera at 22 fps (shutter: 8,

gain: 224, 20x lens). The data were analyzed by Visual SpreadSheet Version 3 and a filter for area-based diameter (ABD > 4µm) was applied. Aspect ratio (> 0.3) and circle fit (> 0.1) were also chosen to exclude impurities with non-circular shapes. No additional filters were applied for derivation of total cell concentration. However, for study of the morphological parameters associated with non-viable cells and subsequent viability determination of different samples, additional filters were used. In order to remove edge particles (particles that were detected at the borders of the camera field, hence imaged partially), the acceptable detection field was reduced to 95 – 1183 and 6 – 952, respectively, for left-right and top-bottom orientations. The edge gradient parameter provided by FlowCAM was used to exclude out-of-focus particles. The acceptable range for edge gradient was determined in a preliminary study. In Table 1, descriptions of the main morphological parameters provided by the Visual SpreadSheet are given. It is worth mentioning that the FlowCAM can calculate the particle size through two different algorithms. In our study we chose to proceed with the area based diameter (ABD) only, because the principle of ABD and ECD is similar.

Fluorescence-activated cell sorting (FACS)

Flow cytometric cell sorting (FACS) on a FACSAria III (BD Biosciences, New Jersey, USA) was used to separate dead and/or dying cells from living cells based on the forward scatter (FSC) and side scatter (SSC) 'live gate' as shown in Supplementary Figure S1. The presumably dead and live cells that were collected with the FACS were then measured with MFI and FlowCAM. These FIM data were used to develop data filters for dead and live cells for each FIM technique. For this purpose the parameter that showed highest difference (for both instruments the size) between live and dead cells, was used as a primary filter. After applying this primary filter, the changes of all the other parameters were monitored. Consequently, threshold values for all the other parameters could systematically be fine-tuned. At the end, the filters were tested on the analyzed sorted fractions and FIM derived viability was compared to the trypan blue assisted values found for each cell sample.

Results

The two B-ALL cell lines were thawed, analyzed and then left at ambient temperature for 8 days and analyzed at predetermined time points, as described in materials and methods.

Monitoring cell concentration over the eight-days study period

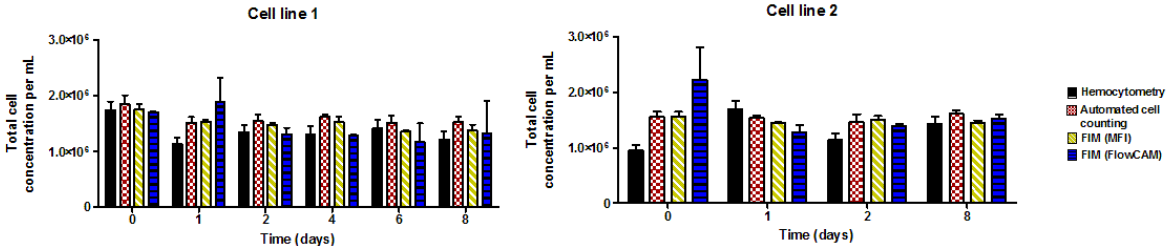

Figure 1: Total cell concentration of (A) cell line 1 and (B) cell line 2 measured at different time points during an 8-day incubation period, as measured by hemocytometry (black), automated cell counting (red), MFI (yellow) and FlowCAM (blue). Error bars represent the standard deviation of triplicate measurements with each technique.

Figure 1 shows the total (live and dead) cell concentrations as measured with all four techniques over the 8-days study period, for both investigated cell lines. The results indicate that all the techniques gave fairly similar cell concentrations. FlowCAM appeared to have the lowest precision, followed by hemocytometry, as judged by the standard deviations. The cell concentration of the cell line 1 showed a decreasing trend over time, whereas for cell line 2 the cell counts remained fairly stable.

Morphological parameters of B-ALL cells monitored with FIM techniques

Both flow imaging microscopy techniques provide morphological parameters of the detected particles (including cells) obtained from the individual images. A few representative images of individual particles detected by the two FIM techniques are shown in Figure 2. It is obvious that FlowCAM has a much higher lens magnification, as seen from the size of the image being larger for the same cell sizes measured with MFI. The high resolution images of FlowCAM compared to MFI may result in the ability to derive more morphological parameters using FlowCAM than MFI. Nevertheless, some of the most relevant parameters allowed a comparison of FlowCAM with MFI (see Table 1). In our 8-days study we monitored changes in all the 5 parameters listed in Table 1 for the studied cells.

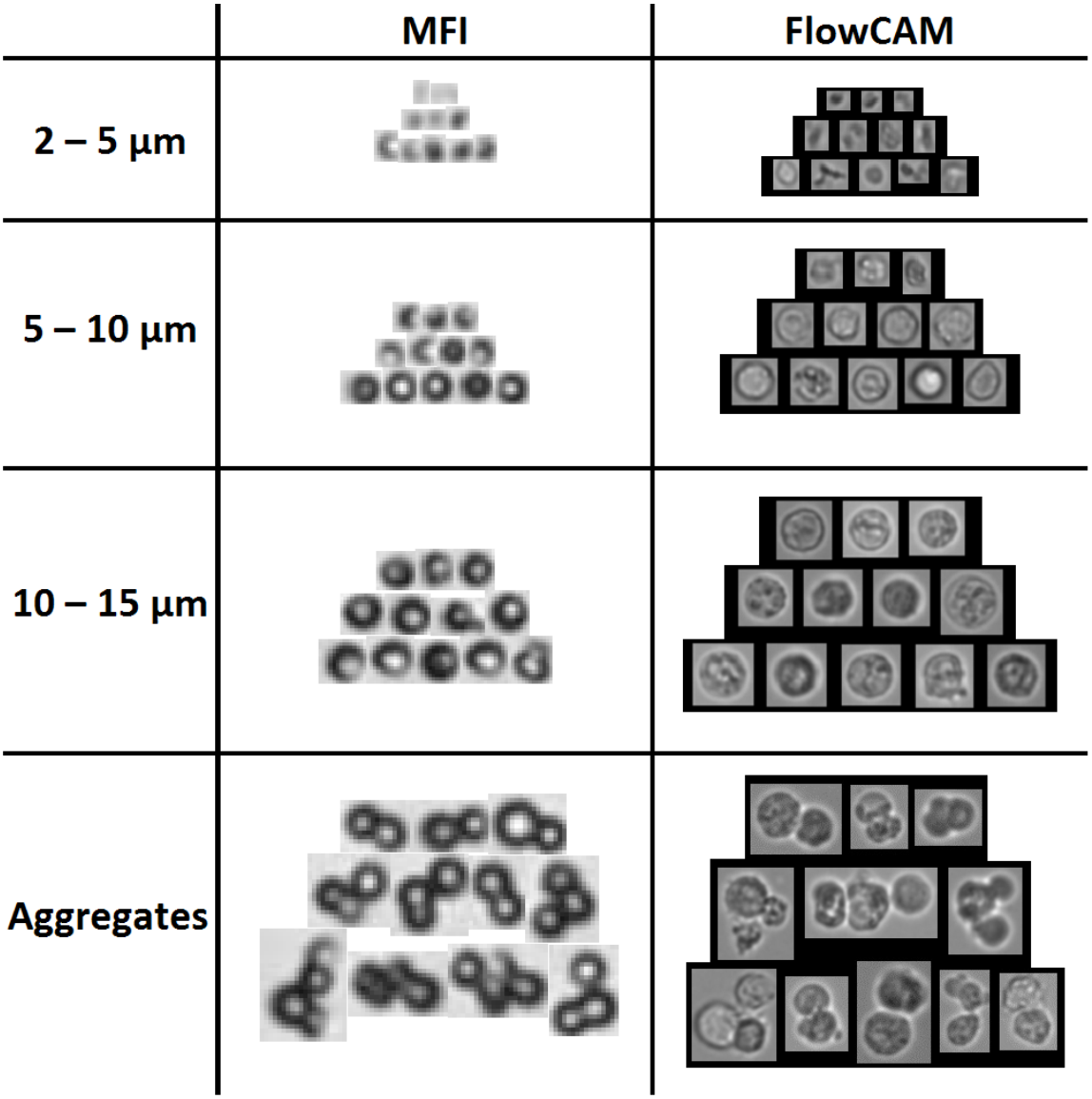

Figure 2: Representative images of the cells detected by MFI (middle column) and FlowCAM (right column). The cells are categorized in three size ranges as shown in the left column.

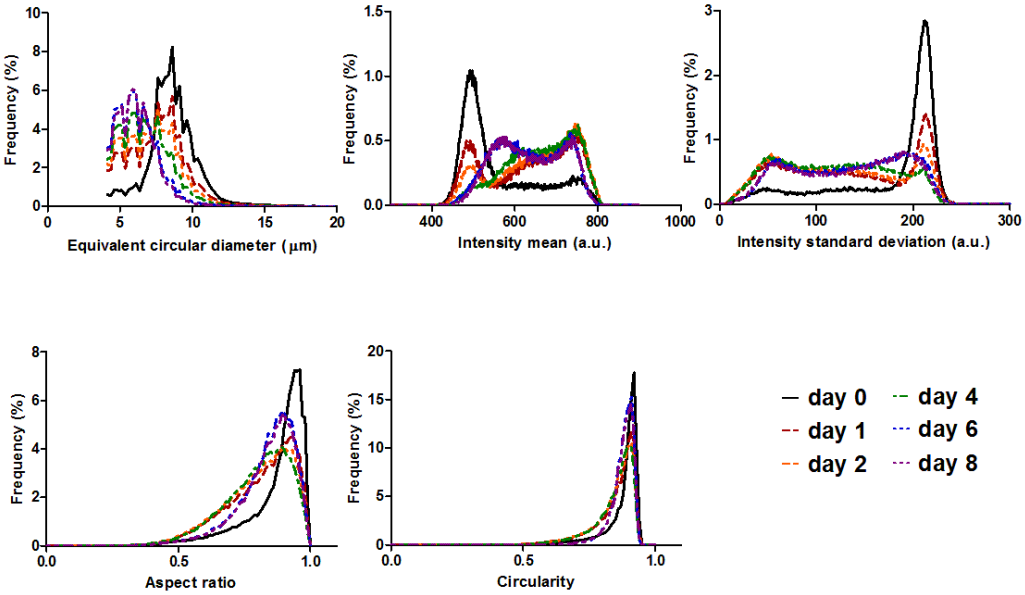

Figure 3: Overview of the changes in different morphological parameters, including size (equivalent circular diameter), of cell line 1, as observed with MFI, during the incubation study. Different line colors represent measurements at different days. For each parameter the frequency distribution of the corresponding parameter unit range is shown.

Figure 3 shows the distribution of particles over the parameters derived from the MFI analysis for cell line 1 during the 8-days incubation study. The size distribution graph shows that there was a decrease in the number of the larger particles and an increase in the number of smaller particles over time. The peak around 8 µm in the distribution of day 1 slowly descended, while a new peak around 6 µm rose and became apparent at day 8. The intensity frequency graphs showed a similar trend. Fresh cell suspension showed pronounced peaks around 490 and 210, respectively, for the mean and standard deviation of intensity. Incubation over time resulted in a decrease of aforementioned peaks and appearance of two other peaks in each graph, namely at 560 and 730 for the mean intensity and at 50 and 180 for the standard deviation of the intensity. For the shape related parameters, *i.e.,* circularity and aspect ratio, only the latter showed distinctive changes in its distribution graph. The aspect ratio value started to decrease and deviated further from 1 over time. The same trend in ECD and intensity mean was observed for cell line 2 (see Supplementary Figure S2). The intensity standard deviation for cell line 2 showed only a decrease and broadening in the main peak, whereas the changes in the shape related parameters were not considerable.

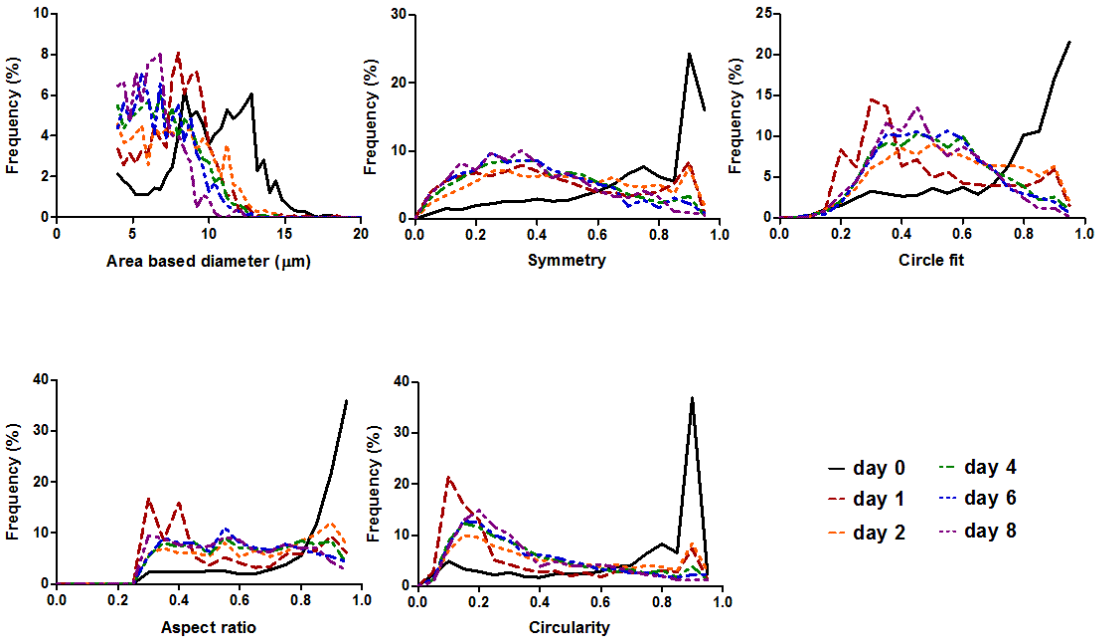

Figure 4: Overview of the changes in different morphological parameters, including size (area based diameter), of cell line 1, as observed with FlowCAM, during the incubation study. Different line colors represent measurements at different days. For each parameter the frequency distribution of the corresponding parameter unit range is shown.

The distribution of particles over the parameters studied with the FlowCAM is shown in Figure 4. The change in the ABD size distribution was fairly similar to the changes seen in the ECD size distribution with MFI. Fresh cell sample showed a distinct peak at about 12 µm and over time this peak disappeared and was replaced by relatively broad peak at a smaller size range (around 6 µm). However, there was also a third transient peak at about 8 µm seen, which was already present in the fresh sample and increased after 24 hours, and then diminished in the following days. In contrast to MFI, with FlowCAM the changes in the particle intensity were not monitored (further explained in the *Discussion* section), and the focus was only put on four shape related parameters. All these parameters showed a distinct peak with a value close to 1 for fresh cell sample, which gradually decreased over days. For symmetry and circle fit a broad peak at about 0.3 and 0.45, respectively, rose and for circularity a narrower peak with a value of 0.2 appeared. Noticeably, for the aspect ratio the frequency distribution did not change considerably after 24 hours of incubation. For cell line 2, all the studied morphological parameters followed a similar trend, although the changes were less pronounced (see Supplementary Figure S3).

Fractionation and FIM derived morphology of dead and live cells

The fresh cell suspension of the first cell line was analyzed with a flow cytometer to derive an appropriate gate for sorting dead and live cells (see Supplementary Figure S1). After the fractions of the dead and live cells as identified by flow cytometry were collected, a control trypan blue assisted viability test of each fraction was performed on the automated cell counter. From these control measurements it was found that the live population contained almost 90% viable cells, whereas the dead population contained no more than 20% viable cells. For comparison, the unfractionated cell population contained about 75% viable cells. The sorted populations were thereafter measured with both FIM techniques to derive the values for the different morphological parameters for live and dead cells separately. The results are shown in Table 2 and indicate that there was a statistically significant difference between the values of each parameter for live and dead cells, except for the circularity values derived from MFI and FlowCAM. The R^2 values indicate the extent of this difference, where a higher R^2 indicates a larger difference between live and dead for that particular parameter. Thereafter, we defined filters based on the monitored parameters for dead and live cells, as shown in Table 3. It has to be noted that although there was no statistically significant difference between the values

Table 2: Derived mean and standard deviation of the morphological parameters provided by MFI and FlowCAM for the two cell fractions of cell line 1 sorted using FACS. The morphological parameters of the dead and live cells are statistically compared, with the results presented in the two rightmost columns.

Flow imaging microscopy morphological parameters*		Live cell population	Dead cell population	Statistical comparison Different?	R^2**
Micro-Flow Imaging					
	ECD	7.6 ± 2.2 µm	5.8 ± 1.8 µm	Yes	0.171
	IntMean	546 ± 87	573 ± 81	Yes	0.026
	IntSD	179 ± 53	173 ± 55	Yes	0.003
	Cir	0.88 ± 0.06	0.88 ± 0.05	No	n.a.
	AR	0.85 ± 0.12	0.87 ± 0.10	Yes	0.008
FlowCAM					
	ABD	7.7 ± 3.0 µm	6.4 ± 2.6 µm	Yes	0.055
	Sym	0.74 ± 0.19	0.69 ± 0.17	Yes	0.019
	AR	0.82 ± 0.16	0.80 ± 0.13	Yes	0.005
	CF	0.77 ± 0.17	0.75 ± 0.13	Yes	0.004
	Cir	0.78 ± 0.17	0.78 ± 0.12	No	n.a.

*Tested morphological parameters: equivalent circular diameter (ECD), intensity mean (IntMean), intensity standard deviation (IntSD), circularity (Cir), aspect ratio (AR), area based diameter (ABD), symmetry (Sym) and circle fit (CF).

**Derived after applying t-test with GraphPad Prism 5®. R^2 quantifies the fraction of all the variations in the samples that is accounted for by a difference between the group means. n.a. = 0.

of circularity for live and dead cells, this parameter appeared to be distinctive (and useful in definition of the FlowCAM filters) when used on top of filters based on other parameters.

Comparing cell viability determination by FIM techniques, hemocytometry and automated cell counting

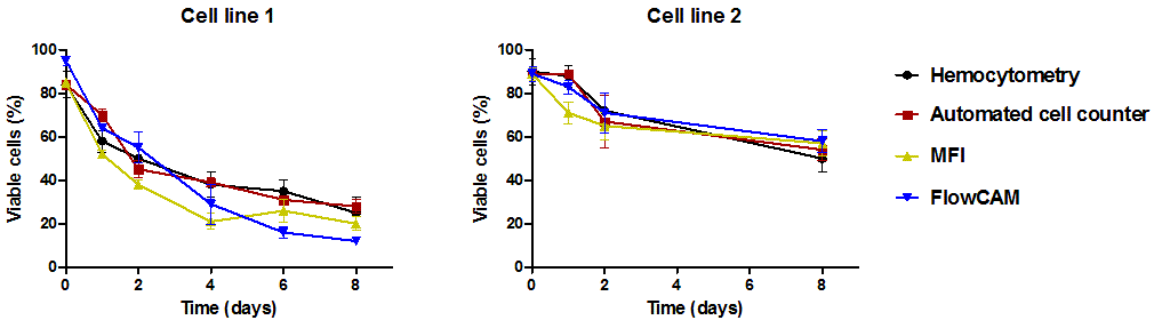

Figure 5: Percentage of viable cells determined with different analytical methods for the cell line 1 at different time points during the 8-day incubation period: hemocytometry (black), automated cell counting (red), MFI (yellow) and FlowCAM (blue). The error bars represent standard deviations of triplicate measurements with each technique.

With the help of the filters for fractionated cells, the percentage of viable cells was calculated for both cells at different time points (Figure 5). These percentages obtained from different techniques showed similar trends for the viability of both cell lines, *i.e.*, a gradually decreasing viability over incubation time. In addition, cell line 2 showed a stronger survival potency at the studied incubation conditions (75% decrease in viable cells after 8 days) than cell line 1 (50% decrease).

Discussion

In clinical practice, where CTPs are required to be checked for concentration and viability prior to administration, a more rapid and easier method would be highly beneficial. In this study we have investigated the potential of two different FIM techniques for this purpose and have shown that both techniques can be used to measure the concentration and the viability of cells, yielding comparable results to those obtained with conventional hemocytometry and cell counting methods.

Table 3: Comparison of the different aspects of the techniques evaluated in this study

Characteristics	Hemocytometry	Automated cell counting	FIM (MFI)	FIM (FlowCAM)
General				
Analyzed sample volume	0.1 µL	0.4 µL	260 µL	20 µL
Sample pretreatment	Labelling; dilution if needed	Labelling; dilution if needed	Dilution	Dilution
Analysis time per sample (measurement + data analysis)	5 minutes	1 minute	15 minutes	10 minutes (depends on measurement settings)
Cell counting and viability determination				
Accuracy	Moderate	Moderate	High	Moderate
Precision	Moderate	Moderate	High	Low
Additional features				
Non-cellular particles	Discarded visually from the cell counts	May interfere with the cell counting	Can be removed from the data afterwards	Can be removed from the data afterwards
Detection of cell debris	Depends on magnification lens used	Not possible	Possible	Possible
Cell identification	Visual identification	Not possible	Possible using morphology based filters	Possible using morphology based filters

The FIM methods, once developed, are easy to perform and do not require staining of the cells before the measurement (see comparison made in Table 3). These techniques measure a large sample volume and thus count considerably more cells than the conventional methods such as hemocytometry. This ability is a great asset for the accuracy and precision of both counting and cell viability determination. Another advantage of FIM lies in its ability to image individual cells and obtain morphological characteristics of each cell. This capability allows avoiding the usage of labels. Moreover, non-cellular materials can be manually removed from the data, to avoid inaccurate counting. Furthermore, the imaging likely allows the discrimination of different types of cells (and/or non-cellular particles) in a heterogeneous population.

Although hemocytometry, automated cell counting, MFI and FlowCAM are all able to provide an estimation of the cell concentration, standard deviations presented in Figure 1 indicate that the precision of methods with respect to the cell concentration measurement follows this pattern FlowCAM < hemocytometry < automated cell Counter < MFI. For FlowCAM the combination of the type of flow cell and image frequencies used in our settings resulted in a theoretical analysis efficiency of around 20%, meaning that only 20% of the dispensed cell suspension was actually imaged. This limitation in combination with the inability of

the analysis package in exclusion of stuck particles that appear in several images from the analysis may be the most important contributing factors to the relatively low precision. Despite the larger amount of suspension volume measured with the automated cell counter, automated cell counting did not show superior precision over hemocytometry with respect to cell concentration. This may be caused by the interference of non-cellular material with the cell counting. In contrast, MFI resulted in the highest precision. The large amount of imaged sample (more than 260 µL vs. 0.1 µL in hemocytometry), high analysis efficiency (about 85%) and ability to remove stuck particles from being counted multiple times may explain the pronounced performance of MFI with respect to the concentration determinations. Moreover, precision of hemocytometry may also be affected by the operator, since the method requires visual counting and viability assessment based on visual discrimination of the color of the cells.

Monitoring of the total concentration of cell line 1 over time revealed a decreasing trend in total cell concentration for all the methods. It is known that the dying and dead cells undergo fragmentation into smaller particles[23]. Presumably these cell debris particles are below the lower size limit of the automated cell counting and the lower size limit chosen for FIM techniques (4 µm), while in hemocytometry non-cellular particles are visually excluded and therefore not counted. FIM data confirm this theory as the ECD and ABD size distribution diagrams (Figure 3 and Figure 4) show a clear increase in the number of particles below 7 µm over time. This increase was even more pronounced for particles below 4 µm, in particular for ECD (Supplementary Figure S4). This observation suggests that the FIM techniques are presumably able to detect and count cell fragments as well. Analysis of the FIM parameters for incubated cells revealed clear changes in the majority of the parameters highlighted in this study, namely ECD, intensity mean, intensity SD and aspect ratio for MFI; and ABD, symmetry, aspect ratio, and circle fit for FlowCAM. Both MFI and FlowCAM revealed a decreasing trend in the size (ECD and ABD, respectively) of the cells during the incubation. Moreover, cells at later time points appeared to have a higher intensity, a lower intensity SD and smaller aspect ratios. The latter, together with lower symmetry and circle fit values, indicate that the shape of the cells changes towards less symmetric and more elongated particles. All these observations point towards a decrease in the population of live cells and/or changes in the quality of the live cell population. Shrinkage of cell size and changes in cell shape are observed for dead and dying cells whose concentration is expected to increase under stress[13]. Furthermore a decrease in the intensity SD can be a sign of disappearance of the cell organelles that contributed to variations in intensity of the image in a cell. In order to investigate if all these changes are correlated, the data from day 1 and 8 were analyzed further by making 3D plots that show the distribution of cells over two MFI derived parameters at the same time (Supplementary

Figure S5). The peak at 480 a.u. in the intensity mean graph of Figure 3 at day 0 belongs to the ECD population around 8 µm (presumably live cells). At day 8 the decrease in cell size and increase in cell intensity result in appearance of a new peak with intensity mean of 730 and ECD of 6 µm (presumably dead cells). Similar changes in other parameters and FlowCAM (Supplementary Figure S6) are observed when the same approach is applied to look into different populations based on size. Overall, these correlated changes in all the morphology parameters for cell population exposed to stress strongly suggest that MFI and FlowCAM are able to pick up early stages of loss in viability that may cause changes in the transparency and shape of the cells[13].

Table 4: Specification of the filters used to identify dead and live cells from analysis results

Flow imaging microscopy morphological parameters		Filter for live cell population	Filter for dead cell population
Micro-Flow Imaging			
	ECD	> 7.25 µm	4 – 7.25 µm
	IntMean	≤ 550	≥ 550
	IntSD	≤ 170	≥ 170
FlowCAM			
	ABD	> 7.0 µm	4 – 9 µm
	Sym	≥ 0.7	≤ 0.8
	AR	≥ 0.8	0.6 – 0.8
	CF	≥ 0.7	≤ 0.8
	Cir	≥ 0.8	0.3 – 0.8

In order to confirm the capability of FIM characterization for identification of live and dead cells and also to define filter conditions that allow quantitative analysis viability separated live and dead cells were obtained by FACS and analyzed. After gating and separation of the two distinct populations as seen in FSC-SCC plot, the live and dead cells were analyzed by both FIM techniques and filter values that allowed distinction of dead from live cells were determined. The filters were constructed by setting one value at a time starting from the most distinctive parameter until no change was observed in the populations. Filter values for MFI data do not include aspect ratio and circularity. After setting the primary filter the values of these two parameters did not change that much between live and dead populations. Filters for FlowCAM, however, included more parameters including circularity. These filters, summarized in Table 4, clearly depict the observations of the incubation experiments. For instance the average size and average intensity are smaller for dead cells.

It has to be noted that the two FIM techniques described herein offer several other morphological parameters that could be used in analysis of the cells. However, the combination of a high-magnification lens and a thin focus plane of the flow cell results in substantial numbers of imaged particles that were out of focus. These particles affect the values of a few morphological parameters (*e.g.*, intensity), and therefore were not included

in our study.

In our study we aimed to develop a label-free FIM based method to derive viability of cells. In order to avoid complexity of the cell sample, we have used a model containing one type of cells, *i.e.*, B-ALL cell lines. However, CTPs may contain cells with different morphological properties than B-ALL cells or contain multiple cell types. For example, different hematopoietic progenitor cell products contain heterogeneous cell population[24]. In principle one can apply the same approach to other cell types and heterogeneous cell populations. Therefore, one needs to develop specific filters for each type of cells.

Conclusion

In this study we have investigated the capability of two different FIM techniques, MFI and FlowCAM, to be used as a label-free method for cell concentration and viability determination. Our data suggests that both methods deliver fairly similar results for concentration and quality determination of cellular products as traditional methods, *i.e.*, hemocytometry and the automated cell counting. Whereas the MFI method showed a higher precision with respect to determination of the cell concentration, the FlowCAM method provides higher-resolution images. The latter may be useful to identify non-cellular particles and potentially discriminate between different types of cells.

References

1. Larijani B, Esfahani EN, Amini P, Nikbin B, Alimoghaddam K, Amiri S, Malekzadeh R, Yazdi NM, Ghodsi M, Dowlati Y, Sahraian MA, Ghavamzadeh A 2012. Stem cell therapy in treatment of different diseases. Acta medica Iranica 50(2):79-96.

2. Mason C, Brindley DA, Cume-Seymour EL, Davie NL 2011. Cell therapy industry: billion dollar global business with unlimited potential. Regen Med 6(3):265-272.

3. Moviglia GA, Vina RF, Brizuela JA, Saslavsky J, Vrsalovic F, Varela G, Bastos F, Farina P, Etchegaray G, Barbieri M, Martinez G, Picasso F, Schmidt Y, Brizuela P, Gaeta CA, Costanzo H, Brandolino MM, Merino S, Pes ME, Veloso MJ, Rugilo C, Tamer I, Shuster GS 2006. Combined protocol of cell therapy for chronic spinal cord injury. Report on the electrical and functional recovery of two patients. Cytotherapy 8(3):202-209.

4. Hickey MJ, Malone CC, Erickson KE, Gomez GG, Young EL, Liau LM, Prins RM, Kruse CA 2012. Implementing preclinical study findings to protocol design: translational studies with alloreactive CTL for gliomas. American journal of translational research 4(1):114-126.

5. Gomez-Lechon MJ, Lahoz A, Jimenez N, Bonora A, Castell JV, Donato MT 2008. Evaluation of drug-metabolizing and functional competence of human hepatocytes incubated under hypothermia in different media for clinical infusion. Cell transplantation 17(8):887-897.

6. Leverett LB, Hellums JD, Alfrey CP, Lynch EC 1972. Red blood cell damage by shear stress.

Biophysical journal 12(3):257-273.
7. Bravery CA, Carmen J, Fong T, Oprea W, Hoogendoorn KH, Woda J, Burger SR, Rowley JA, Bonyhadi ML, Van't Hof W 2013. Potency assay development for cellular therapy products: an ISCT review of the requirements and experiences in the industry. Cytotherapy 15(1):9-19.
8. Strober W 2001. Trypan blue exclusion test of cell viability. Current protocols in immunology / edited by John E Coligan [et al] Appendix 3:Appendix 3B.
9. Panterne BR, M.J., Sabatini C, Ardiot S, Huyghe G, Lemarie C, Pouthier F, Mouillot L. 2011. Ten Years of External Quality Control for Cellular Therapy Products in France. ed.: InTech. p 660.
10. Donner KJ, Becker KM, Hissong BD, Ahmed SA 1999. Comparison of multiple assays for kinetic detection of apoptosis in thymocytes exposed to dexamethasone or diethylstilbesterol. Cytometry 35(1):80-90.
11. Kurec A 2014. Flow cytometry: principles and practices. MLO: medical laboratory observer 46(5):28, 30-21.
12. Sharma DK, King D, Oma P, Merchant C 2010. Micro-Flow Imaging: Flow Microscopy Applied to Sub-visible Particulate Analysis in Protein Formulations. Aaps Journal 12(3):455-464.
13. Matsubayashi M, Ando H, Kimata I, Nakagawa H, Furuya M, Tani H, Sasai K 2010. Morphological changes and viability of Cryptosporidium parvum sporozoites after excystation in cell-free culture media. Parasitology 137(13):1861-1866.
14. Tsaousis KT, Kopsachilis N, Tsinopoulos IT, Dimitrakos SA, Kruse FE, Welge-Luessen U 2013. Time-dependent morphological alterations and viability of cultured human trabecular cells after exposure to Trypan blue. Clinical & experimental ophthalmology 41(5):484-490.
15. Wu L, Martin T, Li Y, Yang L, Halpenny M, Giulivi A, Allan DS 2012. Cell aggregation in thawed haematopoietic stem cell products visualised using micro-flow imaging. Transfus Med 22(3):218-220.
16. Farrell CJ, Cicalese SM, Davis HB, Dogdas B, Shah T, Culp T, Hoang VM 2016. Cell confluency analysis on microcarriers by micro-flow imaging. Cytotechnology.
17. Werk T, Volkin DB, Mahler HC 2014. Effect of solution properties on the counting and sizing of subvisible particle standards as measured by light obscuration and digital imaging methods. European Journal of Pharmaceutical Sciences 53:95-108.
18. Frahm GE, Pochopsky AW, Clarke TM, Johnston MJ 2016. Evaluation of Microflow Digital Imaging Particle Analysis for Sub-Visible Particles Formulated with an Opaque Vaccine Adjuvant. PloS one 11(2):e0150229.
19. Zolls S, Weinbuch D, Wiggenhorn M, Winter G, Friess W, Jiskoot W, Hawe A 2013. Flow imaging microscopy for protein particle analysis--a comparative evaluation of four different analytical instruments. The AAPS journal 15(4):1200-1211.
20. Weinbuch D, Zolls S, Wiggenhorn M, Friess W, Winter G, Jiskoot W, Hawe A 2013. Micro-flow imaging and resonant mass measurement (Archimedes)--complementary methods to

quantitatively differentiate protein particles and silicone oil droplets. Journal of pharmaceutical sciences 102(7):2152-2165.

21. Nijmeijer BA, Szuhai K, Goselink HM, van Schie ML, van der Burg M, de Jong D, Marijt EW, Ottmann OG, Willemze R, Falkenburg JH 2009. Long-term culture of primary human lymphoblastic leukemia cells in the absence of serum or hematopoietic growth factors. Exp Hematol 37(3):376-385.

22. Louis KS, Siegel AC 2011. Cell viability analysis using trypan blue: manual and automated methods. Methods in molecular biology 740:7-12.

23. Kerr JFR, Wyllie AH, Currie AR 1972. Apoptosis - Basic Biological Phenomenon with Wide-Ranging Implications in Tissue Kinetics. Brit J Cancer 26(4):239-&.

24. Services USDoHaH. 2016. Cellular & Gene Therapy Products: Marketed Products. ed.

Supplementary Information

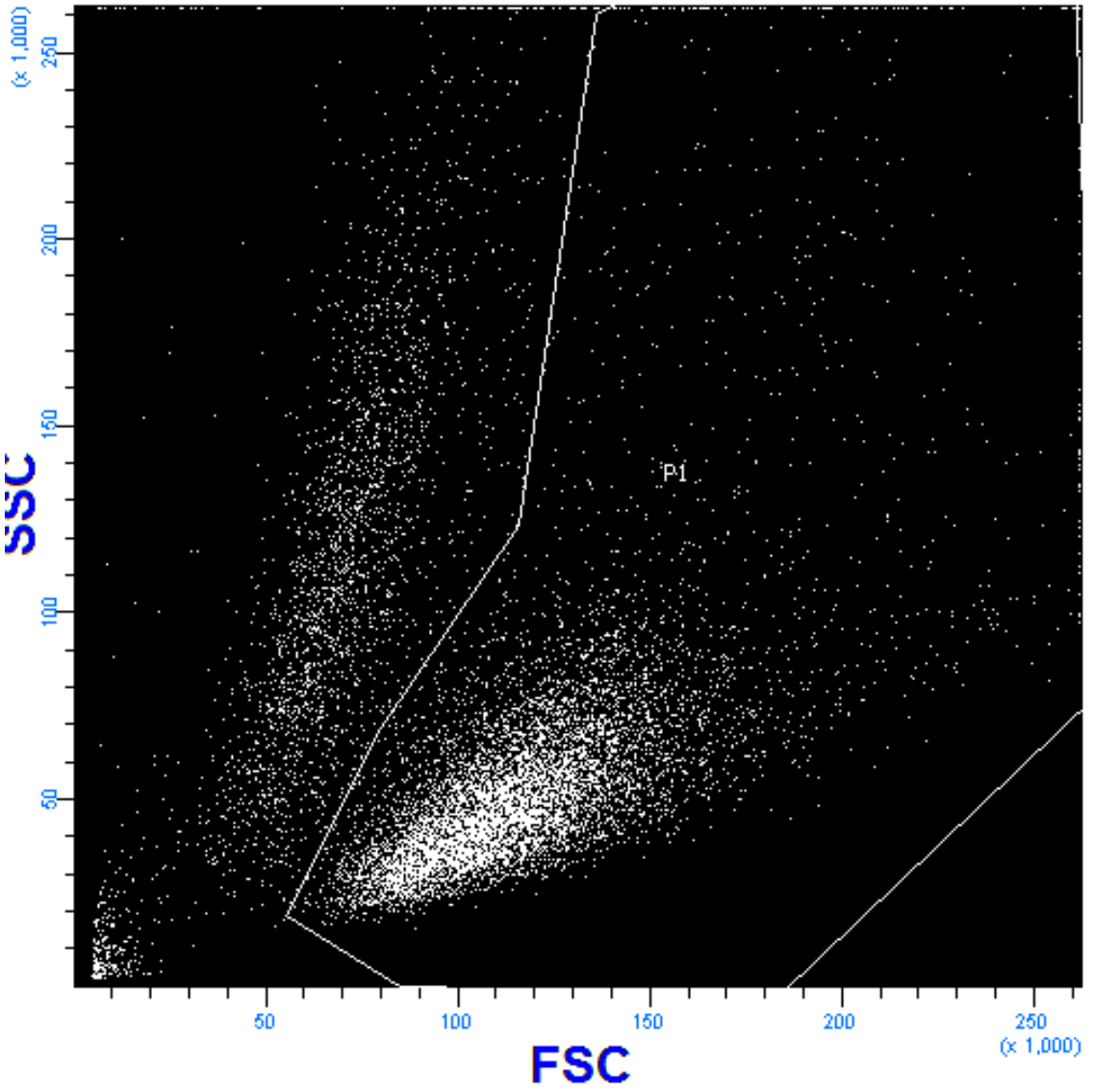

Supplementary Figure S1: Gating strategy for the FACS supported sorting of dead/ dying and viable cells. The graph shows the FSC – SSC plot for the sample containing fresh cells from cell line 1. The gated population is considered viable.

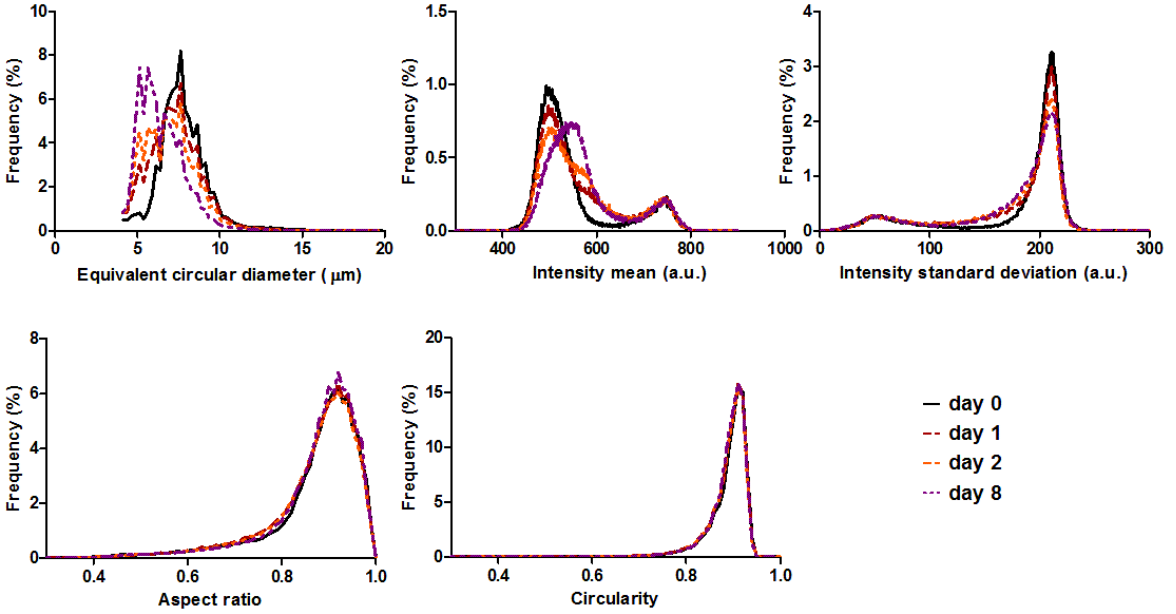

Supplementary Figure S2: Overview of the changes observed in different morphological parameters as function of incubation time of cell line 2, as observed with MFI, during the incubation study. For each parameter the frequency distribution of the corresponding parameter unit range is shown.

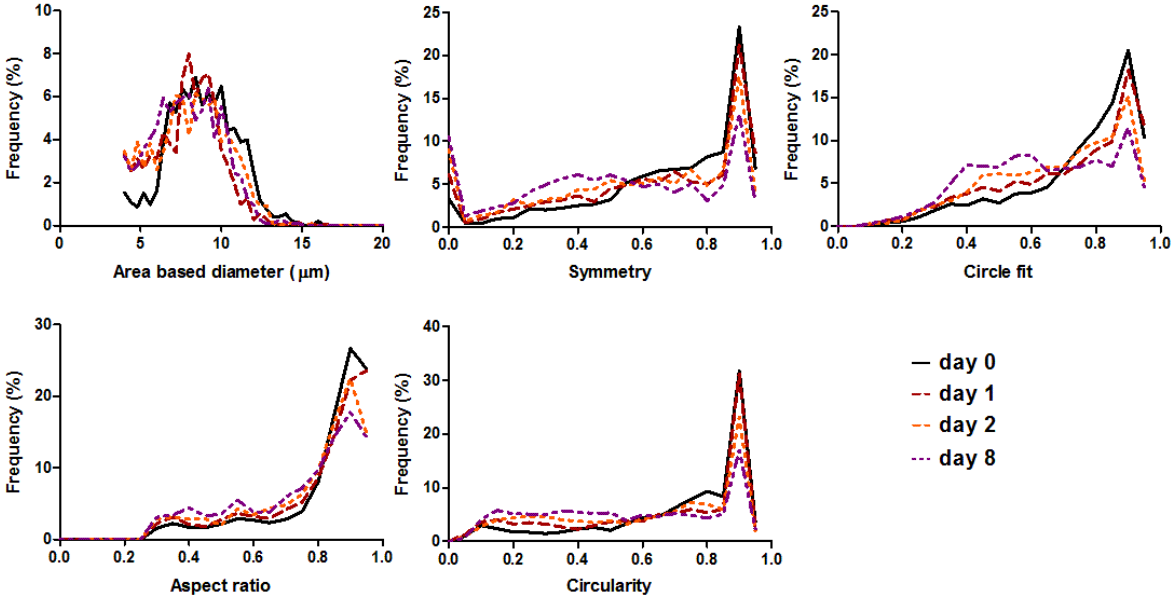

Supplementary Figure S3: Overview of the changes observed in different morphological parameters as function of incubation time of the cell line 2, as observed with FlowCAM, during the incubation study. For each parameter the frequency distribution of the corresponding parameter unit range is shown.

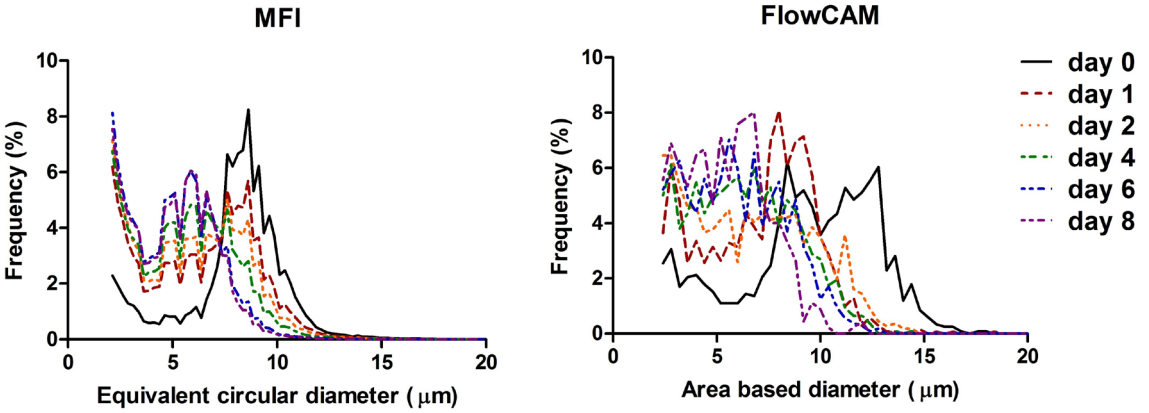

Supplementary Figure S4: Changes in MFI and FlowCAM sizing parameters, of cell line 1, during the incubation study.

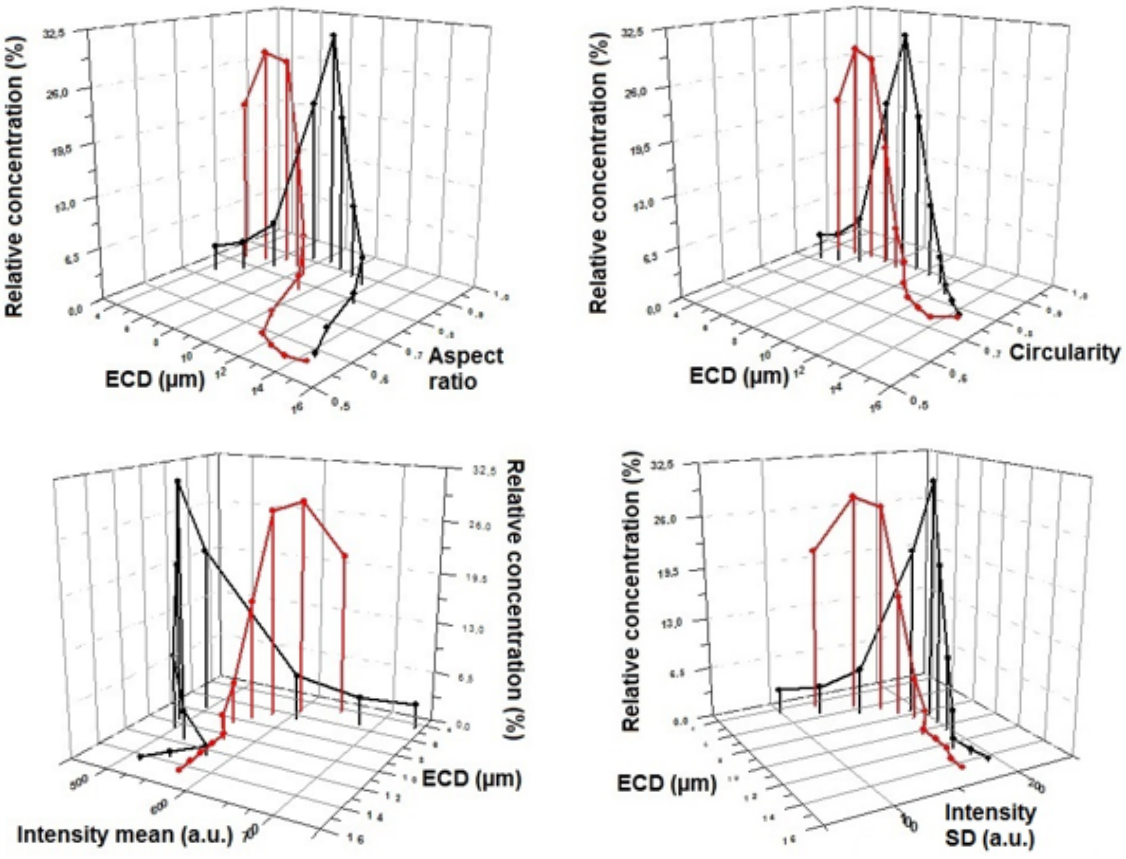

Supplementary Figure S5: Overview of the MFI derived aspect ratio, circularity, average intensity and SD intensity for different ECD-based size populations. The x-axis in all the graphs shows these populations as 1-µm size bins (from 4 – 15 µm). The y-axis presents the concentration of each 1-µm size bin populations relative to the total concentration. In the z-plane the average values of different morphological parameters for each size-based population is shown. The results for samples of fresh cells (in black) and cells incubated for 8 days at ambient conditions (in red) are shown.

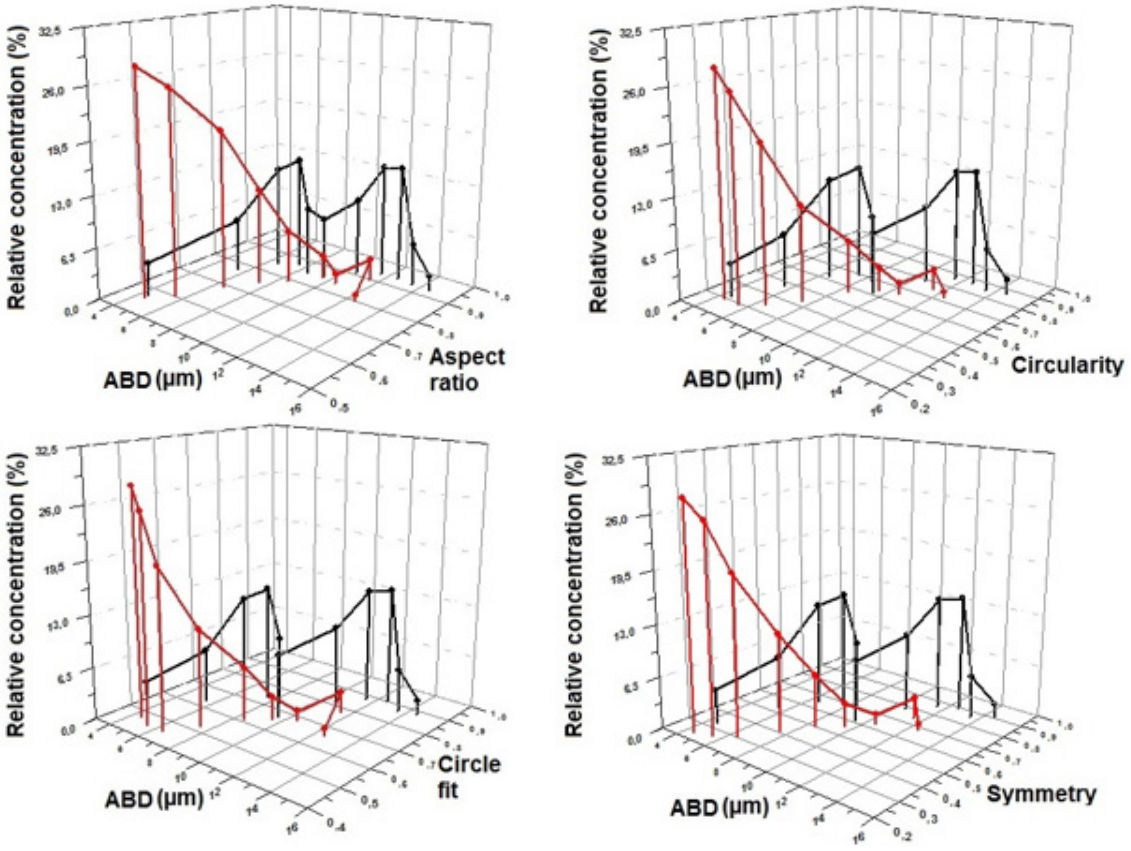

Supplementary Figure S6: Overview of the FlowCAM derived aspect ratio, circularity, circle fit and symmetry for different ABD-based size populations. The x-axis in all the graphs shows these populations as 1-µm size bins (from 4 – 15 µm). The y-axis presents the concentration of each 1-µm size bin populations relative to the total concentration. In the z-plane the average values of different morphological parameters for each size-based population is shown. The results for samples of fresh cells (in black) and cells incubated for 8 days at ambient conditions (in red) are shown.